ChemCatChem

Research Article
doi.org/10.1002/cctc.202401118

Chemistry Europe
European Chemical Societies Publishing

www.chemcatchem.org

Toward a Generic Model for Phosgene Synthesis Catalysis over Activated Carbon

Rory Hughes,[a] Philip R. Davies,[b, c] Colin Brennan,[d] and David Lennon*[a]

A reaction model was recently been postulated to describe the phosgene synthesis process over an activated carbon catalyst. That body of work exclusively considered a single grade of activated carbon (Donau Supersorbon K40), raising the issue that the mechanistic insight gleaned could be restricted to the single substrate. Therefore, to evaluate the generality of the proposed sequence of elementary reactions that lead to phosgene production, this article concentrates on Norit RX3 Extra, a representative activated carbon that finds wide application in industrial applications. Several phosgene synthesis traits were associated with Donau Supersorbon K40 and are reproduced with Norit RX3 extra over the reaction conditions studied, such as exclusive phosgene selectivity and a degree of reagent retention. However, temperature-programmed reaction studies show the reaction profile of the Norit RX3 extra to exhibit deviations from that observed for Donau Supersorbon K40. A modified reaction model is proposed to account for these differences. The revised reaction model is thought to represent a generic model for phosgene synthesis that can accommodate disparities in the surface chemistry of different activated carbon formulations.

1. Introduction

Phosgene ($COCl_2$) is a widely manufactured compound with uses in the polymer, pharmaceutical, and agrochemical industries.[1–4] The global production of phosgene is on the scale of 12 Mt per annum,[5] and is estimated to rise to 18.6 Mt per annum by 2030.[4] The vast majority of the global capacity of phosgene is utilized in the production of isocyanates and polycarbonates.[4] For these industrial applications, phosgene formation is almost an exclusively produced from the reaction of carbon monoxide and dichlorine over an activated carbon catalyst.[6]

$$CO_{(g)} + Cl_{2(g)} \xrightarrow{cat} COCl_{2(g)}$$

There is a paucity of studies of phosgene synthesis in the open literature. The lack of in-depth study of a commercially relevant system is attributable to two operational constraints. Firstly, the study of phosgene synthesis is hindered by the significant chemical hazards of the reagents and products.[2,7,8] Secondly, the study of the highly carbonaceous catalysts via optical spectroscopy is challenging.[9,10,11] Despite these operational hurdles, there are a handful of studies of the carbon catalyzed $COCl_2$ synthesis reaction, as outlined below.

In 1920 Atkinson and co-workers showed phosgene could be synthesized from activated carbon at temperatures as low as 14 °C, while also noting that dissociation of phosgene product begins to occur at 200 °C; an important consideration for such an exothermic reaction ($\Delta H = -107.6$ kJ mol^{-1}).[1] Furthermore, they noted that a small excess of CO as compared to Cl_2 yielded a product stream free from chlorine, a methodology that is now accepted standard industrial practice.[1] In their studies of $COCl_2$ synthesis, Potter and Barron[12,13] used Langmuir–Hinshelwood expressions to account for observed temporal trends.[12] Later, in 1970, Csűrös and co-workers have investigated the effect of a nitrogen diluent on the reaction system.[14] In a series of papers between 1974 and 1979, Shapatina and co-workers[15–17] have also applied Langmuir–Hinshelwood reaction kinetics to the reaction system and reported that the activated carbon catalyst retained chlorine, indicating that not all chlorine introduced to the catalyst is reacted to form phosgene.[15]

Over the period of 1980 to 2000, there appears to be a break in the reporting of $COCl_2$ synthesis in the academic literature, although the patent literature remained fairly active.[18–23] In 2000, Abrams and co-workers studied the formation of the carbon tetrachloride (CCl_4) byproduct.[24] Using ^{13}C labelled CO, the researchers suggested that CCl_4 formation occurs by over-chlorination of the catalyst, rather than by disproportionation of the $COCl_2$. In 2001, Ajmera and co-workers were described a multichannel micro packed bed reactor design, with an empha-

[a] R. Hughes, Prof. D. Lennon
School of Chemistry, Joseph Black Building, University of Glasgow, Glasgow G12 8QQ, UK
E-mail: David.Lennon@glasgow.ac.uk

[b] P. R. Davies
School of Chemistry, Cardiff University, Main Building, Park Place, Cardiff CF10 3AT, UK

[c] P. R. Davies
HarwellXPS, ESPRC National Facility for X-ray Photoelectron Spectroscopy, Research Campus at Harwell, Didcot OX11 0FA, UK

[d] C. Brennan
Syngenta, Jealott's Hill International Research Centre, Bracknell, Berkshire RG42 6EY, UK

[Correction added on 26 December 2024, after first online publication: The copyright line was changed.]

Supporting information for this article is available on the WWW under https://doi.org/10.1002/cctc.202401118

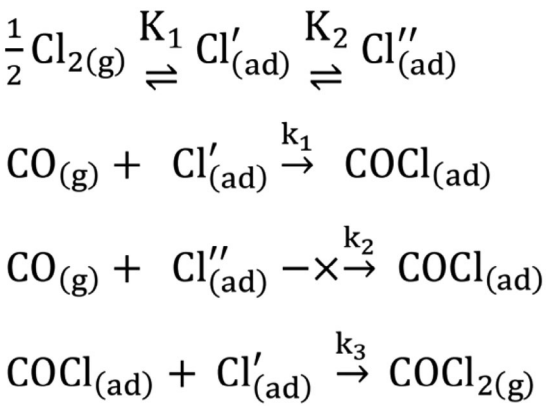

Scheme 1. The proposed reaction model for phosgene synthesis from the carbon monoxide and chlorine, over the Donau Supersorbon K40 activated carbon catalyst at 323 K. The graphic is reproduced from ref. [21] with permission from the publisher (Elsevier).

sis on increasing operator safety.[25] Later, in 2012, Mitchell and co-workers examined a range of commercially available activated carbon catalysts for their phosgene synthesis ability.[1] In a series of papers investigating phosgene synthesis over various graphene-based structures, Gupta and co-workers suggested that sp^2 hybridized carbon is responsible for phosgene synthesis,[26–28] and that phosgene synthesis can be enhanced over graphene-based structures by the addition of nitrogen-doping. In contrast to the findings of Potter and Baron, an Eley–Rideal type mechanism was proposed to account for the trends observed over these substrates. Over the period of 2018 to 2020, Bähr and co-workers reported an experimental apparatus[29] for testing synthesized mesoporous carbon materials that can adsorb and desorb larger quantities of chlorine than a commercially available catalyst.[30]

Supplementing these studies, Rossi and co-workers described the use of a commercially available catalyst that were previously considered by Mitchell and co-workers, Donau Supersorbon K40, for phosgene synthesis.[31–34] Two types of chlorine adsorption to the catalyst are proposed: one that is active for the synthesis of phosgene and one which is not; with the latter site retaining chlorine post reaction. Scheme 1 presents the reaction model proposed by Rossi and co-workers for phosgene synthesis over Donau Supersorbon K40. K_1 and K_2 are equilibrium constants, respectively, associated with the dissociative adsorption of chlorine into active (Cl′) and inactive (Cl′) surface sites. k_1 is a rate coefficient associated with the collision of gaseous carbon monoxide with chlorine atoms adsorbed at active sites. k_2 is a rate coefficient associated with the collision of gaseous carbon monoxide with chlorine atoms adsorbed at the inactive sites; this reaction does not proceed under the specified reaction conditions. k_3 is a rate coefficient associated with the concerted formation of phosgene at active sites and the simultaneous desorption into the gaseous phase.[34]

As Rossi and co-workers[31–34] have focused on only a single catalyst formulation, Donau Supersorbon K40, the authors conceded that the associated reaction model (Scheme 1) might only be applicable to this specific formulation of activated carbon.[34] Against this background, the present communication looks to assess the reaction mechanism with respect to a different catalyst formulation, namely Norit RX3 Extra. This material is intended to represent a typical phosgene synthesis catalyst,[1] and, as such, is deemed suitable to assess the generality of the surface chemistry outlined in Scheme 1. Both the Norit RX3 Extra formulation of activated carbon were utilized in this study and the Donau Supersorbon K40, utilized by Rossi and co-workers,[31–34] were analyzed by the Mitchell and co-workers.[1] Thus, the primary objective of the current study is to evaluate whether the mechanistic detail evident in Scheme 1 is applicable to another candidate phosgene synthesis catalyst, that is, Norit RX3 Extra.

Given the wider use of phosgene as a reagent in the chemical manufacturing industry,[2–4] the work addresses a driver for a greater understanding and applicability of activated carbons were deployed for phosgene synthesis. Firstly, a physical characterization of the Norit RX3 Extra sample examined is presented. Secondly, the sample is analyzed for phosgene synthesis. The work directly follows on from a recent publication by us, that describes the up-dated phosgene test apparatus that is used alongside a range of operational procedures that reflect the hazardous nature of the reaction system under investigation.[7]

2. Experimental Section

2.1. Characterization

Thermogravimetric analysis (TGA) and derivative gravimetric analysis (DTG) were performed on a TA Instruments SDT Q600. The gas flowed over the sample was 2% O_2/Ar at a flow rate of 100 mL/min, and the temperature was ramped from 293 to 1273 K at a rate of 10 K/min. Scanning electron microscopy with an energy dispersive x-ray spectroscopy (SEM/EDX) analysis was performed on a Philips/FEI XL30 ESEM Microscope fitted with an Oxford Instruments Energy 250 energy dispersive spectrometer. The microscope was operated at an electron acceleration voltage of 25 kV and utilized a x-act 10 mm^2 silicon drift detector. EDX measurements were taken at three different sites per sample and the results were averaged.

X-ray photoelectron spectroscopy (XPS) was acquired using a Kratos Axis SUPRA with monochromated Al kα (1486.69 eV) X-rays at 15 mA emission and 12 kV HT over an analysis area of 700 × 300 µm. CasaXPS (version 2.3.25)[35] was used to analyze the spectra with binding energies referenced to the large graphitic carbon component in the C(1 s) region at 284.7 eV. Nitrogen adsorption isotherm experiments were determined the surface area of the activated carbon using a quantachrome quadrasorb evo instrument. The sample were underwent a degassing procedure for 16 h at 383 K under an argon atmosphere prior to nitrogen adsorption at 77 K.

Raman spectroscopy was performed using a Horiba Jobin Yvon LabRAM HR with a Ventus 532 nm 100 mW laser. The measurements were taken at a laser grating of 600 gr/mm with a hole size of 200 µ and a laser strength of 10%, observing the sample over the energy range of 100–2000 cm^{-1}.

Powder x-ray diffraction (XRD) analysis was performed on a Rigaku MiniFlex benchtop diffractometer, equipped with a Cu Kα radiation source. The sample was scanned between 20 and 90° at a rate of 0.07° per min.

2.2. Catalyst Testing

2.2.1. Standard Operating Conditions

The reactor configuration was used to investigate the Donau Supersorbon K40 activated carbon, which was amended to examine the Norit RX3 Extra under consideration here, as comprehensively described recently.[7] The operation involved charging the reactor (outer diameter 6.35 mm, quartz) with 0.1250 g of catalyst (Norit RX3 Extra Activated Carbon, reference 901934–500 G), ground to between 250 and 500 μm by using sieves (endcotts). Prior to the reaction and in the presence of flowing nitrogen, the sample was dried for 16 h at 373 K with heating provided by a temperature-controlled oven (TF1 11/32/150, Carbolite Gero).

The flow of gasses were employed in this study utilized a slight excess of CO compared to Cl_2 (CO, 5 mL/min, Cl_2 4 mL/min), to mimic industrial operation.[1] The carrier gas utilized was N_2 at 50 mL/min, corresponding to a space velocity over the reactor of 8725 h^{-1}. A further 100 mL/min N_2 was introduced postreactor to ensure products remained in the gas phase. This corresponded to 159 mL/min total flow through the infrared (Is10, Nicolet) and ultraviolet/visible (UV-1800, Shimadzu) spectrometers, were used for analysis of the reactor exit gasses. The flow of the gasses was metered by mass flow controllers (CO, and N_2 –HFC-202, Cl_2–HFC-302 (Hastings) operating from a CCD104 controller display (Chell)). At each sampling interval, four spectra were recorded in series and peak areas averaged. The standard deviation of these four peaks was then used to estimate errors in the measurement. The acquisition times for a single IR and UV–vis spectrum were 1 and 2 min respectively, leading to 4 and 8 min for the individual spectral acquisition times; this corresponds to an overall spectral acquisition period of 8 min for a single datapoint in the reaction profiles.

2.2.2. Isothermal Reaction as a Function of Time

The flow of the gasses was set-up for 1 h over a bypass reactor containing the quartz equal in volume to the standard 0.1250 g, 250–500 μm catalyst (0.41 cm^3, 0.4410 g).[32] The bypass reactor was held outside the temperature-controlled oven and maintained at room temperature. Previous studies have shown that $COCl_2$ synthesis does not occur over ground quartz in this arrangement after 300 min time on stream at 323 K.[7] Furthermore, under the same flow regime, no $COCl_2$ synthesis was detected at temperatures as high as 673 K.[32] However, it cannot be discounted that thermal-mediated homogenous $COCl_2$ synthesis[36] may have contributed to $COCl_2$ synthesis in the catalyst-containing reactor, under reaction conditions. While this bypass arrangement did not allow for estimation of a potential homogeneous contribution, it did allow the reaction gasses to be set up in an equivalent flow regime to that found in the catalyst-containing reactor. After 1 h, A_0 measurements were taken in the absence of the catalyst, after which the flow of gas was directed over the catalyst containing-reactor, maintained at 323 K. Samples were taken in 30 min increments for 300 min, including at 0 min.

2.2.3. Reaction as a Function of Temperature

The flow of reagents and diluent gas was allowed to set-up for 1 h over a bypass reactor containing ground quartz. After 1 h, A_0 measurements were taken in the absence of the catalyst, after which the flow of gas was diverted over the reactor containing the catalyst. The reaction was run at a given temperature for 1 h, allowing steady-state conditions to be achieved.[33] After the spectroscopic measurements were complete, the temperature was increased in 15–20 K steps between 333 and 504 K, and allowed to react for a further hour between each temperature step.

3. Results and Discussion

3.1. Catalyst Characterization

3.1.1. Chemical Characterization

The chemical nature of the surface groups were presented on an activated carbon surface typically play a significant role in both the catalytic and adsorption characteristics of a given activated carbon.[37] However, as discussed in the introduction, analysis of these surface groups by optical spectroscopy poses an operational challenge.[9] One technique which can probe the nature of the surface of activated carbon is gravimetric analysis. TGA and DTG analysis was performed on fresh Norit RX3 Extra ground to 250–500 μm (Figure S1). For TGA, 4.6 mg of the 14.3 mg sample remained at 1273 K, representing 31.8% of the starting material, indicating that approximately a third of the starting material remains thermally stable in the presence of an oxidizing environment. The DTG plot reveals a peak at ~340 K, which is thought to correspond to the removal of physisorbed water.[38] Beyond this, several smaller peaks can be identified between 450 and 650 K that are attributed to the decomposition of surface functional groups; thought to be carboxylic acids, carboxylic anhydrides, and lactone groups.[39,40] A large peak was centred around 1050 K is attributed to the decomposition of the bulk activated carbon material.[37] In addition to this bulk decomposition, at elevated temperatures, >873 K, more stable surface functionalities, such as carbonyl, phenol, and quinone groups, are decomposed.[39,40] Surface oxides, such as carboxylic acids and phenolic moieties, have been shown to interact with gas phase chlorine.[41,42]

Further analysis of the activated carbon can be provided by probing the nature of the residual chemical species. EDX is a convenient form of elemental analysis,[43] although it does not convey information on bonding environment. Figure S2 presents the EDX spectrum of Norit RX3 Extra, while Table 1a presents the EDX-derived elemental composition of the sample. Oxygen is present at 2.2 wt%, which compares to previously reported values of 3.9[44] and 4.5 wt%;[45] oxygen can be present on the activated carbon surface in many forms, including carboxylic acid, carbonyl, and phenyl groups.[39,40]

Inspection of Table 1, Sample (a) shows that elements such as chlorine, sulfur, aluminum, and silicon can be found in trace amounts, totalling 2.1 wt%. These elements are often termed as "ash",[37,44,45] and are thought to be the result of incomplete removal of chemical activation agents in the manufacturing process.[37] Such ash heteroatoms are not thought to be associated with chlorine retention; rather, it is thought that a selection of oxygen containing surface groups as well as surface hydrogen and olefinic and graphitic carbon are responsible for the chlorine adsorption.[26,41,42,46]

Some information on the specific environment of the oxygen and carbon atoms in activated carbon can be determined by using XPS. Unlike EDX, XPS does convey information on the

Table 1. Table of elements were found by SEM/EDX and XPS analysis of Norit RX3 Extra.

Sample	Carbon (wt%)	Oxygen (wt%)	Chlorine (wt%)	Sulfur (wt%)	Aluminum (wt%)	Silicon (wt%)
(a) EDX pre reaction	95.9 ± 0.3	2.2 ± 1.9	0.9 ± 1.0	0.9 ± 0.7	0.1 ± 0.1	0.2 ± 0.3
(b) EDX post reaction	91.5 ± 0.6	2.7 ± 0.6	4.9 ± 0.4	0.3 ± 0.01	0.5 ± 0.5	–
(c) XPS pre reaction	81.6 ± 1.0	9.0 ± 1.0	–	0.6 ± 1.0	–	1.8 ± 1.0

Sample (a) represents as-received Norit RX3 Extra. Sample (b) represents a post reaction sample of Norit RX3 Extra, after experiencing the following reaction conditions: CO and Cl_2 flow rates of 5 mL/min and 4 mL/min, respectively, in a 150 mL/min flow of N_2 (50 mL/min prereactor, 100 mL/min postreactor) at 323 K over a timescale of 300 min. (c) Elemental composition of the untreated Norit surface calculated from the XP spectra.

bonding environment of the atoms identified, although XPS is limited to conveying information on surface functionality as the technique's penetration depth is typically of the order of 10 nm.[47] Figure S3a,b presents the O1s and C1s spectra of as-received Norit RX3 Extra, respectively. The O(1s) spectrum (Figure S3a) suggests the presence of hydroxyl and carboxyl surface functionality with peaks at 531.7 and 533.1 eV respectively,[48,49] both of which have been proposed to play a role in chlorine adsorption.[46] Lower binding energy features at 529.0 and 530.3 eV are probably oxides associated with the ash residue. XPS shows a higher concentration of oxygen to reside at the surface (Table 1). In the C(1s) spectrum, (Figure S3b) the strong low binding energy feature at 284.7 eV and associated satellite features (~291 eV) suggests the presence of ordered graphitic carbon, which may have a role in the adsorption of chlorine.[28] The feature at 282 eV is a Ru contaminant associated with the sample mount, it was not seen in the EDX data and can be ignored. Finally, Figure S3c,d shows some of the ash residues present in this sample of Norit RX3 Extra, specifically silicon and sulfur, consistent with EDX analysis (Table 1). Thus, XPS analysis identifies the presence of surface functionalities reported to be responsible for chlorine adsorption.[28,46] As considered in the introduction, it is believed that surface bound chlorine is the key reagent in phosgene synthesis.[34] However, other functionalities such as isolated olefinic bonds and surface hydrogen, which have also been shown to adsorb chlorine,[42,46] have not been identified through any of the techniques as discussed in this section.

3.1.2. Structural Characterization

The structural characteristics of a catalyst formulation can have a large impact on its activity. Activated carbon catalysts typically possess surface areas in excess of 1000 m^2/g.[50] Mitchell and co-workers have tested a series of activated carbon materials (with surface areas ranging from 890 m^2/g to 1250 m^2/g) against a mesoporous activated carbon with a surface area of 325 m^2/g.[1] This mesoporous catalyst have showed greatly reduced activity for $COCl_2$ synthesis as a function of temperature. As such, there may be some structure-activity relationship for activated carbon catalysts in $COCl_2$ synthesis.[51] Figure S4 presents the BET adsorption isotherm[51] for Norit RX3 Extra, ground to 250–500 μm. The form of the isotherm presented conforms to Type I, or Langmuir type, which is indicative of a microporous solid.[52,53] The BET surface area calculated from this measurement is 1397 m^2/g; a value comparable to BET surface areas typically quoted for Norit RX3 Extra (1100–1550 m^2/g).[45,54–62] The micropore volume was calculated via the T-plot method was found to be 0.47 cm^3/g, which typically ranges from 0.47 cm^3/g to 0.49 cm^3/g in the literature for Norti RX3 Extra.[1,45,55,56] In addition, the total pore volume was found to be 0.55 cm^3/g, in good agreement with literature values which ranges from 0.54 cm^3/g to 0.59 cm^3/g for Norit RX3 Extra.[1,45,54–56]

Raman Spectroscopy commonly finds application in determining the graphitization of highly carbonaceous materials.[63–65] Furthermore, some publications have suggested that the large graphitic structures may be the active site for $COCl_2$ synthesis, using highly ordered carbon nanostructures as a proxy for activated carbons.[26–28] Figure S5 presents the Raman spectrum of Norit RX3 Extra, which exhibits two intense features were centred around 1331 and 1588 cm^{-1}. These are indicative of K phonons of A_{1g} symmetry (D-bands) and zone centre phonons of E_{2g} symmetry (G-bands), respectively.[63–66] The ratio of the D-band peak height compared to G-band peak height can be used to give an indication of how ordered a given carbonaceous sample is,[64] termed the I_D/I_G ratio.[32,64,66,67] Activated carbons, which are inherently amorphous compared to graphite,[68] typically have I_D/I_G ratios, ranging from 0.90 to 1.39.[32,67,68] As such, the value derived from Figure S4 of 1.15 fits within previously reported values for this material.

A final method of characterization were adopted in this study is powder XRD.[69] Figure S6 presents the XRD diffractogram of Norit RX3 Extra, where two broad features can be observed, centred around 23° and 43° 2θ. These features are indicative of amorphous carbon.[32] There is no evidence of any features related to inorganic ashes, consistent with the low ash content of this activated carbon (Table 1). These findings are comparable with the previously reported XRD diffractograms of Norit RX3 Extra.[55,62,70]

The combination of Raman and XRD analysis suggests that Norit RX3 Extra may be classified as an amorphous carbon, rather than a highly graphitic carbon. Furthermore, Section 3.1.1 shows that the material exhibits a range of sites and chemical environments that could support the chlorine adsorption and phosgene formation. Nonetheless, the specific identification of "active sites" for phosgene synthesis catalysis alludes us currently.

3.2. Reaction as a Function of Time

Carbon monoxide and chlorine were passed over the catalyst at a temperature of 323 K for a duration of 300 min. Figures 1 and 2

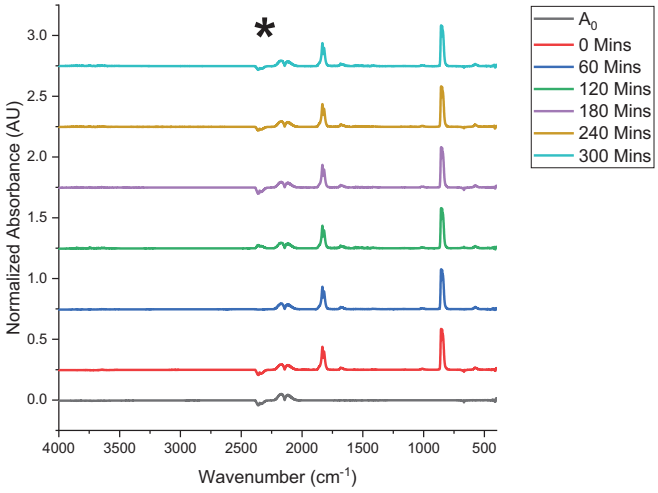

Figure 1. Infrared spectra of reactor exit stream when CO and Cl_2 are passed over 0.1250 g of Norit RX3 Extra activated carbon catalyst, ground to 250–500 µm, with respective flow rates of 5 mL/min and 4 mL/min in a 150 mL/min flow of N_2 (50 mL/min prereactor, 100 mL/min postreactor) at 323 K, over a timescale of 300 min. A_0 corresponds to the by-pass reactor, 0.4410 g of quartz, ground to 250–500 µm at 293 K. The asterisk denotes the presence of atmospheric CO_2 at 2350 cm^{-1}, that is not associated with the reaction system.

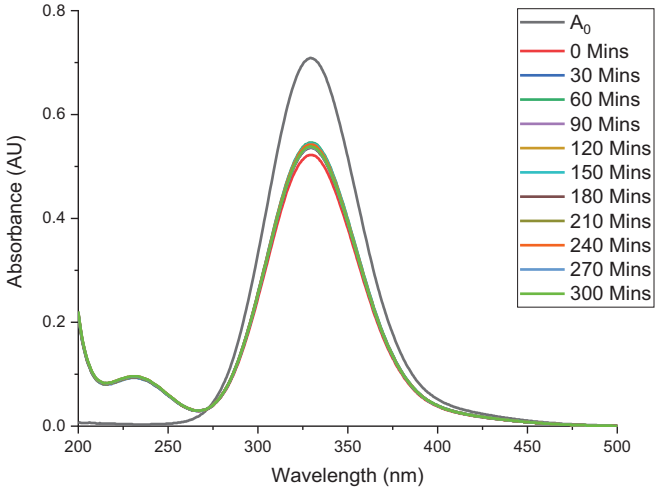

Figure 2. UV–vis spectra of the reactor exit stream when CO and Cl_2 are passed over 0.1250 g of Norit RX3 Extra activated carbon catalyst, ground to 250–500 µm, with respective flow rates of 5 mL/min and 4 mL/min in a 150 mL/min flow of N_2 (50 mL/min prereactor, 100 mL/min postreactor) at 323 K over a timescale of 300 min. A_0 corresponds to the bypass reactor, 0.4410 g of quartz, ground to 250–500 µm at 293 K.

present the resulting IR and UV–vis spectra, respectively. Figure 1 shows the features at around 2350 cm^{-1} that are attributed to a small level of CO_2 breakthrough from the spectrometer purge system, with the atmospheric contaminant contained within the spectrometer optical path but not present within the reaction cell.[71] From the initial A_0 taken over ground quartz, only one feature is present, at around 2140 cm^{-1}, which is attributed to CO.[32] When the reagent flow is passed over the catalyst, it can be seen that intense features were emerge at around 1825 and 845 cm^{-1}. These are assigned to the ν_1(C—O) and ν_4(C—Cl) modes of phosgene, respectively.[2] Furthermore there is a reduction in the intensity of the CO feature at 2140 cm^{-1}. There are several less intense features that was present in these spectra, which are attributable to combination and overtone bands of phosgene,[2] as well as atmospheric water within the spectrometer optical path but external to the reaction gases.

Inspection of Figure 2 (UV–vis spectroscopy) yields similar conclusions to Figure 1. In the initial A_0 spectrum, the only feature present is centred around 330 nm that is attributed to chlorine.[32] When the reagent mixture is passed over the catalyst, the intensity of this peak diminishes. Furthermore, a feature emerges at 230 nm, which is attributable to phosgene.[32] While there are variations in the intensity of the peak centred around 330 nm, these are not systematic and are believed to result from minor fluctuations in the feed stream. In a previous publication,[7] we estimated the overall error in measuring the phosgene synthesis process as being ±5.5%. This error was attributed to fluctuations in the delivery of gasses by the mass flow controllers and spectral acquisitions by the spectrometers. Additionally, it is accepted that some fluctuations may occur via the chlorine interaction with the walls of the apparatus. As such, it is suggested that Norit RX3 Extra readily produces phosgene from carbon monoxide and chlorine under the given conditions. Moreover, no by-products are detected by either spectroscopic method. The by-product which is ubiquitously synthesized by an industrial-scale $COCl_2$ reactors is carbon tetrachloride, CCl_4.[19,20,24,72–74] In the vapour-phase, this molecule exhibits an intense band at 795 cm^{-1} in the IR spectrum.[75] As can be seen from Figure 1, while the ν_4(C—Cl) feature of $COCl_2$ is close in proximity at 845 cm^{-1}, no signal attributable to CCl_4 is detected during this reaction. The absence of any detectable by-products in Figures 1 and 2 indicates that the reaction system has 100% relative selectivity for phosgene under the stated conditions.

Quantification of the spectra presented in Figures 1 and 2, as described in a recent publication,[7] allows for the conversion of peak area into a flow rate (in terms of millimoles of reagent/product per minute normalized to catalyst mass). Figure 3 presents the resulting reaction profile, which shows phosgene formation to rapidly achieve steady-state operation; it is being effectively instantaneous on the timescale of the measurement process (*ca.* 8 min). No deactivation of the catalyst is apparent over the course of this 300 min reaction. Taking the final 300 min sample as representative of steady-state performance, the phosgene formation rate is 0.33 mmol/min/$g_{(cat)}$. This corresponds to a reagent conversion of 9.3%, from 1.92 and 1.39 mmol/min/$g_{(cat)}$ of CO and Cl_2 respectively, for a total reagent flow of 3.31 mmol/min/$g_{(cat)}$. A reagent conversion of 9.3% is purposefully low, both to reduce the chemical hazard posed by $COCl_2$,[7] and to aid kinetic analysis.[76] There is also a notable differential in the adsorption profile of the two reagents (i.e., higher adsorption for Cl_2 than CO, which has also been noted over Donau Supersorbon K40[34]), which may affect the stoichiometric balance. The phosgene production rate exceeds that reported for Donau Supersorbon K40 recorded at the same temperature (0.17 mmol/min/$g_{(cat)}$), with the higher rate for Norit RX3 Extra thought to reflect the revised reactor configuration adopted here (Section 2.2.1). Overall, Figure 3 reproduces the

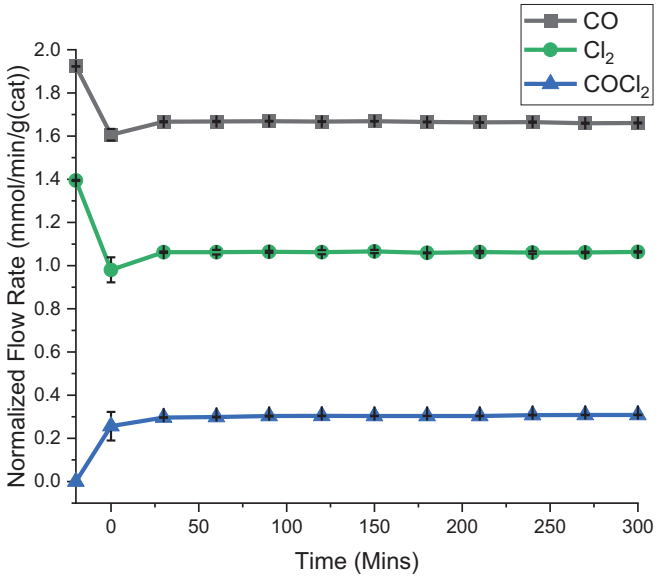

Figure 3. Reaction profile of CO and Cl_2 passed over 0.1250 g of Norit RX3 Extra activated carbon catalyst, ground to 250–500 µm, with respective flow rates of 5 mL/min and 4 mL/min in a 150 mL/min flow of N_2 (50 mL/min prereactor, 100 mL/min postreactor) at 323 K over a timescale of 300 mins. t = −20 min (A_0) corresponds to the by-pass reactor, 0.4410 g of quartz, ground to 250–500 µm at 293 K. The error bars represent the standard deviation of four samples recorded in series.

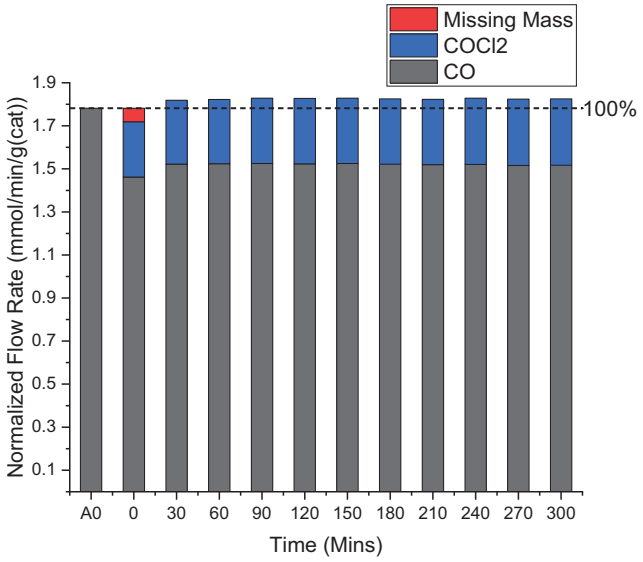

Figure 4. Mass balance plot of CO and $COCl_2$, when CO and Cl_2 passed over 0.1250 g of Norit RX3 Extra activated carbon catalyst, ground to 250–500 µm, with respective flow rates of 5 mL/min and 4 mL/min in a 150 mL/min flow of N_2 (50 mL/min prereactor, 100 mL/min postreactor) at 323 K over a timescale of 300 min. A_0 corresponds to the by-pass reactor, 0.4410 g of quartz, and ground to 250–500 µm at 293 K. The black dashed line indicates the initial A_0 value of carbon monoxide, 1.92 mmol/min/$g_{(cat)}$, which is labeled as 100%.

general trends observed for isothermal phosgene production over Donau Supersorbon K40.[33]

Figures 4 and 5 present the associated carbon and chlorine mass balance profiles, respectively. Figure 4 shows a slight mass excess of carbon monoxide from ~30 min time on stream. Taking 300 min as the representative of the entire reaction course, this excess is + 2.4% of the initial CO A_0 measurement. Given that the estimated experimental error in this measurement is of the order of ± 5.5%,[7] Figure 4 is interpreted as indicating the isothermal reaction profile (Figure 3) as returning a closed carbon mass balance.

The equivalent chlorine mass balance profile (Figure 5) shows a noticeable mass imbalance at short reaction times, but under steady-state conditions, as signified by the values at 300 min, this has reduced to −1.7% of the initial Cl_2 A_0 value. Although within the precision of the measurement (± 5.5%),[7] for reaction times of ≥30 min, Figure 5 shows this small chlorine imbalance to be effectively constant and systematic, suggesting that, in contrast to the carbon profile (Figure 4), there is indeed a small and continuous retention of chlorine during steady-state phosgene production at 323 K. This deduction is backed up by SEM/EDX analysis of a postreaction sample (Section 3.1.1, Table 1, Sample (b), Figure S7) that returns a chlorine content value of 4.9 wt%, which compares to the prereaction value of 0.9 wt% (Table 1, Sample(a)). As previously discussed, no by-product formation is observed in this reaction system. While some chlorine is suggested here to be retained by the catalyst, and thus reduces conversion to $COCl_2$, the relative selectivity for the product $COCl_2$ is maintained at 100%. Under comparable reaction conditions, Rossi and co-workers reported a chlorine deficit of 9.6% of the total chlorine flow rate for Donau Supersorbon K40.[33] Therefore,

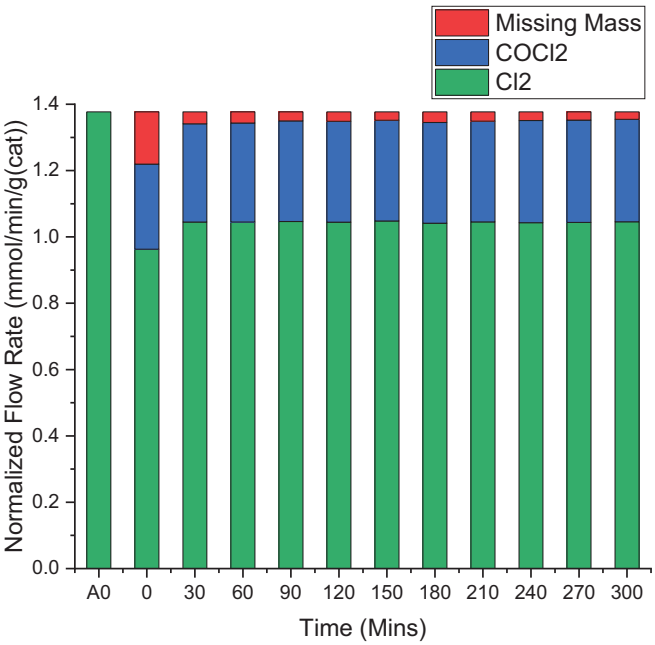

Figure 5. Mass balance plot of Cl_2 and $COCl_2$ when CO and Cl_2 passed over 0.1250 g of Norit RX3 Extra activated carbon catalyst, ground to 250–500 µm, with respective flow rates of 5 mL/min and 4 mL/min in a 150 mL/min flow of N_2 (50 mL/min prereactor, 100 mL/min postreactor) at 323 K over a timescale of 300 min. A_0 corresponds to the by-pass reactor, 0.4410 g of quartz, and ground to 250–500 µm at 293 K.

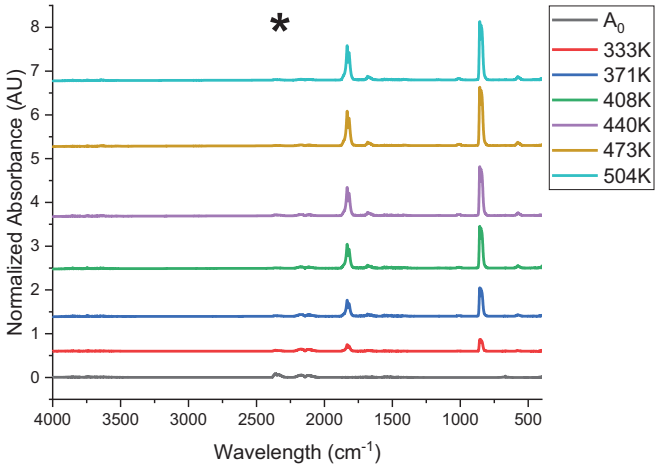

Figure 6. Infrared spectra of CO and Cl_2 passed over 0.1250 g of Norit RX3 Extra activated carbon catalyst, ground to 250–500 µm, with respective flow rates of 5 mL/min and 4 mL/min in a 150 mL/min flow of N_2 (50 mL/min prereactor, 100 mL/min postreactor), over a temperature range of 333–504 K. A_0 corresponds to the by-pass reactor, 0.4410 g of quartz, and ground to 250–500 µm at 293 K. The asterisk denotes the presence of atmospheric CO_2 at 2350 cm^{-1}, which is believed to not be part of the reaction system.

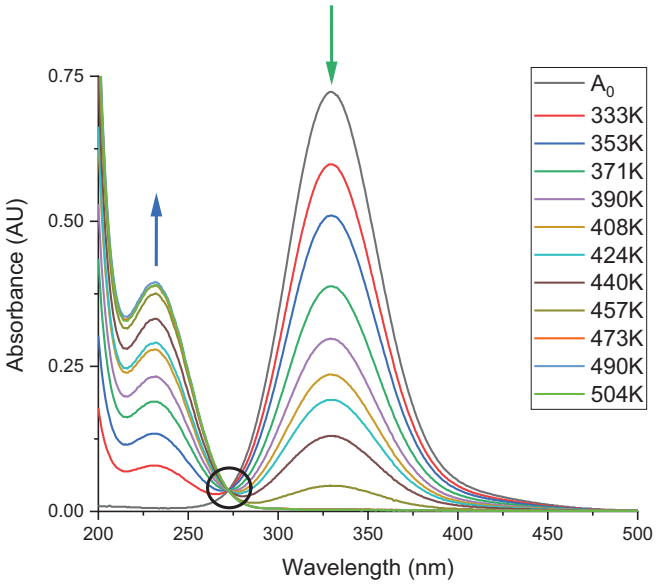

Figure 7. UV–vis spectra of CO and Cl_2 passed over 0.1250 g of Norit RX3 Extra activated carbon catalyst, ground to 250–500 µm, with respective flow rates of 5 mL/min and 4 mL/min in a 150 mL/min flow of N_2 (50 mL/min prereactor, 100 mL/min postreactor) over a temperature range of 333–504 K. A_0 corresponds to the by-pass reactor, 0.4410 g of quartz, ground to 250–500 µm at 293 K. The green arrow indicates the progressive consumption of chlorine; the blue arrow indicates the progressive production of phosgene, with respect to increasing temperature. The black circle at around 270 nm represents an isosbestic point.

both Donau Supersorbon K40 and Norit RX3 Extra retain chlorine during reaction at 323 K, the extent of this retention is noticeably reduced for the latter material.

3.3. Reaction as a Function of Temperature

The reaction was followed as a function of temperature between 333 and 504 K; Figures 6 and 7 show the corresponding IR and UV–vis spectra. Figure 6 shows the intense signals were attributed to phosgene, at 1825 and 845 cm^{-1},[2] to increase as a function of temperature. Accordingly, the signal attributed to carbon monoxide at 2140 cm^{-1}[32] concomitantly diminishes, indicating increasing the consumption of the reagent on increasing temperature. Other than slight atmospheric carbon dioxide and water breakthrough from the spectrometer purge unit (as discussed in Section 3.2.), no other chemical species are detected in these spectra.

Considering the thermal stability of activated carbons, temperature-programmed analysis in the presence of oxygen is reported in the academic[1] and patent literature.[20] While the oxidizing power of oxygen differs from chlorine, thermal analysis in oxygen is thought to represent a suitable proxy for chlorine. Inspection of the TGA data were produced over Norit RX3 Extra (Figure S1), shows the sample to be oxidatively and thermally stable until approximately 850 K. Therefore, over the temperature range studied in this section (333 K to 504 K), significant decomposition of the catalyst is not a feature. Moreover, it is noted that the duration of these temperature-programmed experiments was *ca*. 11 h and throughout, no deactivation of the catalyst was observed. Therefore, it is deduced that Norit RX3 Extra is a durable catalyst formulation for the target reaction.

Inspection of Figure 7 leads to the similar conclusions to those deduced from the IR spectra. The absorption associated with chlorine, 330 nm,[32] progressively diminishes as a function of temperature. At 473 K, the chlorine signal is completely absent, that is, complete dichlorine conversion at $T \geq 473$ K. Similarly, inspection of the signal associated with phosgene, at 230 nm,[32] increases as a function of temperature. At a temperature of 473 K, the phosgene signal plateaus, indicating that phosgene production does not increase beyond this temperature. No chemical species other than chlorine and phosgene are evident in these spectra.

Quantification of the spectra were presented in Figures 6 and 7 allows for the creation of the reaction profile that is presented in Figure 8, which shows the consumption of reagents and the formation of phosgene. When no chlorine can be detected exiting the reactor, the consumption of carbon monoxide and production of phosgene are also plateau. Carbon monoxide is not fully consumed, as an excess flow of this reagent is employed to mimic typical industrial operating conditions.[1]

Figures 9 and 10 present the associated carbon and chlorine mass balance profiles, respectively. Concentrating first on the carbon mass balance, Figure 9 shows a seemingly random fluctuation within the temperature range 333–457 K that varies between +0.9 and +0.33% of the CO A_0 value. However, over the higher temperature range of 473–504 K, there appears to be a small but systematic mass imbalance. For example, at 504 K this accounts for a carbon deficit of −2.5% of the original CO flow rate. These deviations are from 100%, which are small and within experimental error but, on the basis of systematic trends observed, they are interpreted to indicate a closed carbon mass

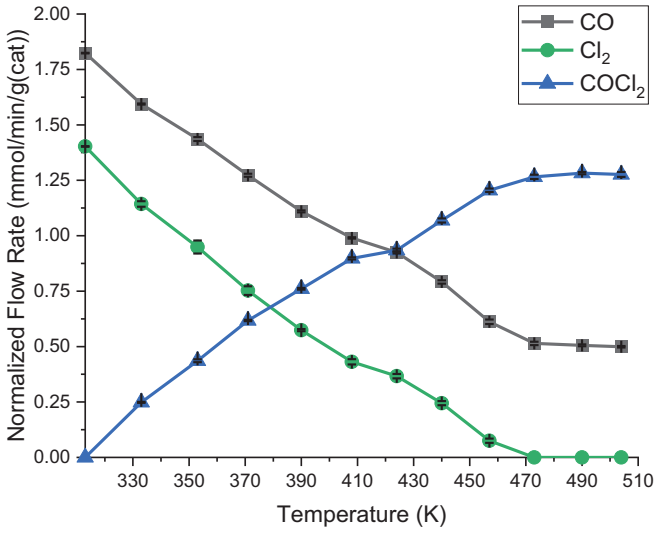

Figure 8. Reaction profile of CO and Cl_2 passed over 0.1250 g of Norit RX3 Extra activated carbon catalyst, ground to 250–500 µm, with respective flow rates of 5 mL/min and 4 mL/min in a 150 mL/min flow of N_2 (50 mL/min prereactor, 100 mL/min postreactor) over a temperature range of 333–504 K. A_0 (320 K) corresponds to the by-pass reactor, 0.4410 g of quartz, and ground to 250–500 µm at 293 K. The error bars superimposed on the symbols represent the standard deviation of four samples recorded in series.

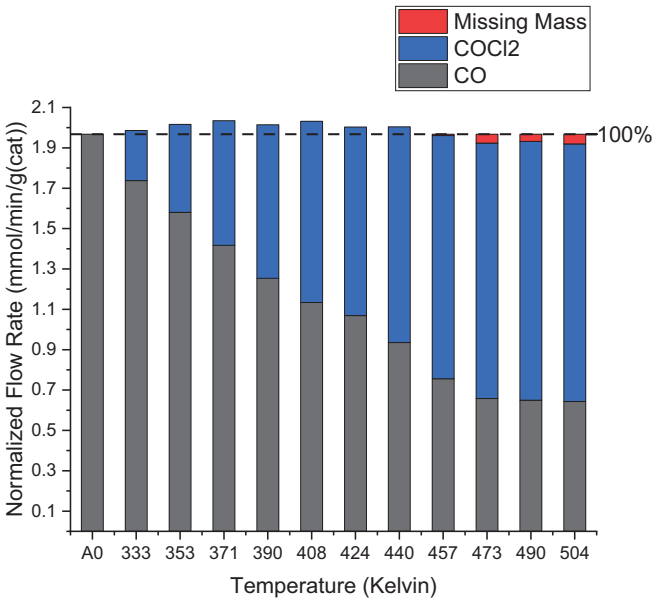

Figure 9. Mass balance plot of CO and $COCl_2$, when CO and Cl_2 are passed over 0.1250 g of Norit RX3 Extra activated carbon catalyst, ground to 250–500 µm, with respective flow rates of 5 mL/min and 4 mL/min in a 150 mL/min flow of N_2 (50 mL/min prereactor, 100 mL/min postreactor) over a temperature range of 333–504 K. A_0 (320 K) corresponds to the by-pass reactor, 0.4410 g of quartz, and ground to 250–500 µm at 293 K. The black dashed line indicates the initial A_0 value of carbon monoxide (1.96 mmol/min/$g_{(cat)}$), which is labeled as 100%.

balance for T $\leq$ 457 K but for T $\geq$ 473 K, a small carbon imbalance is observed. This CO retention at elevated temperatures may indicate an activated process. However, given that the CO mass imbalance is small (−2.5%, Figure 9) against a significant $COCl_2$ production rate (~1.27 mmol/min/$g_{(cat)}$, Figure 8), the CO retention pathway is viewed as a minority occurrence under these conditions.

Figure 10 shows the situation with the temperature-programmed chlorine mass balance profile to be more distinct than that of the carbon mass balance, with an evident mass imbalance ultimately exceeding systematic experimental error. At 333 K, a slight chlorine deficit of 0.8% of the incident chlorine molar flow rate (A_0) is observed. However, as the temperature is increased, this imbalance systematically increases, so that the molar chlorine flow rate at 504 K represents −11.3% of the chlorine A_0 value, establishing that substantial chlorine retention is evident during phosgene production at temperatures of 500 K or thereabouts.

It is evident from Figure 10 that increasing temperature leads to increasing chlorine conversion up to 473 K, when complete conversion is achieved. As Figure 7 shows no chlorine is returned to the gas phase at these elevated temperatures, it is thought that the 11% chlorine imbalance reflects the chlorine retained at type II sites, that is, $Cl''_{(ad)}$ of Scheme 1.

Interestingly, Figure 8 shows that despite this degree of chlorine retention, the phosgene formation rate is maintained at ~1.27 mmol/min/$g_{(cat)}$ over the range 473–504 K, that is, the chlorine retention is not inducing catalyst deactivation for this set of reaction conditions. As mentioned in the Introduction, CCl_4 formation may be linked to a catalyst deactivation process, with the by-product formation proposed to occur via over-chlorination

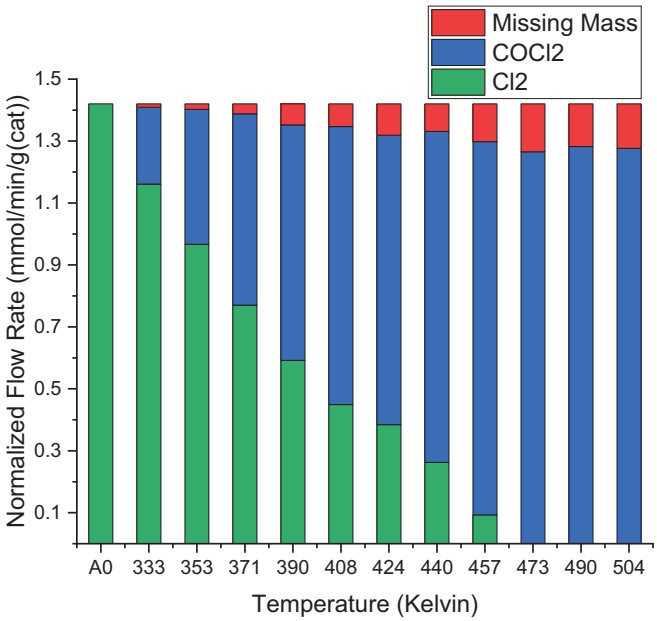

Figure 10. Mass balance plot of Cl_2 and $COCl_2$, when CO and Cl_2 are passed over 0.1250 g of Norit RX3 Extra activated carbon catalyst, and ground to 250–500 µm, with respective flow rates of 5 mL/min and 4 mL/min in a 150 mL/min flow of N_2 (50 mL/min prereactor and 100 mL/min postreactor) over a temperature range of 333–504 K. A_0 (320 K) corresponds to the by-pass reactor, 0.4410 g of quartz, and ground to 250–500 µm at 293 K.

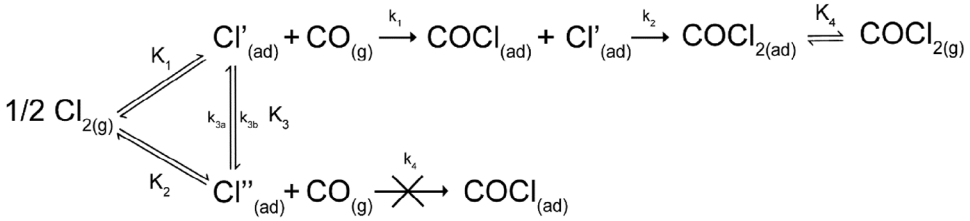

Scheme 2. A modified reaction model for phosgene synthesis from carbon monoxide and chlorine over activated carbon. The model newly incorporates k_{3a} and k_{3b} to allow for the different activated carbons to present different chlorine surface inter-site diffusion rates, whilst the introduction of k_4 accounts for the phosgene desorption from the activated carbon surface.

of the catalyst at elevated temperatures,[20,24,72,73] rather than via disproportionation of the $COCl_2$ product. As such, it cannot be discounted that the retained chlorine may represent a precursor to CCl_4 formation, which has not fully met the thermal or oxidative requirements for synthesis. As such, the issue of CCl_4 formation in $COCl_2$ synthesis are required in further study.

In a qualitative sense, Norit RX3 Extra is exhibiting similar attributes with regards phosgene synthesis catalysis to that observed with Donau Supersorbon K40 for the range of reaction conditions examined:[32,33] (i) a degree of chlorine retention during phosgene production, (ii) effectively complete phosgene selectivity (no gaseous by-products detected), (iii) rapid achievement of steady-state operation, and (iv) there is no evidence for catalyst deactivation. However, Figure 8 does exhibit some discrimination. For Donau Supersorbon K40, Rossi and coworkers report an activation energy for phosgene synthesis of 34.1 ± 0.2 kJ mol^{-1}[33] and a temperature-programmed reaction profile that displays complete consumption of a chlorine feed rate of 4 mL min^{-1} occurring at 393 K.[32] Moreover, an increased phosgene production rate is observed over the temperature range of 393–423 K, which corresponds to the total chlorine consumption.[32] Further heating to 445 K leads to no further increase in phosgene production, which plateaus at 1.42 mmol min^{-1} $g_{(cat)}{}^{-1}$. With reference to Scheme 1, this outcome was rationalized via an equilibrium existing between active adsorbed chlorine atoms ($Cl_{(ad)}{}'$), and an inactive adsorbed chlorine atoms ($Cl_{(ad)}{}''$). Equation (1) specifies this stage:

$$Cl'_{(ad)} \underset{\rightleftharpoons}{K_2} Cl''_{(ad)} \tag{1}$$

where K_2 represents the associated equilibrium constant. Specifically, it was proposed that the back reaction was active over the range 393–423 K, which provided the source of active chlorine that could then react with incident CO molecules to form product.[32] This scenario does not pertain to Norit RX3 Extra. Firstly, Norit RX3 Extra exhibits an activation energy for phosgene synthesis of 43.0 ± 1.1 kJ mol^{-1}[7] (8.9 kJ mol^{-1} higher than observed for Donau Supersorbon K40). Secondly, for the same incident catalyst mass normalized incident chlorine flow rate, complete chlorine consumption is not achieved until 473 K (80 K higher than observed for Donau Supersorbon K40). A further important distinction were between the two materials is that Figure 8 shows the phosgene flow rate to plateau at 473 K, corresponding to the point of complete chlorine conversion. Thus, despite the presence of excess CO, no more phosgene production is evident over the region 473–504 K. Whereas Figure 10 shows a fraction of the chlorine consumed (11%) is retained by the catalyst over this temperature range, Figure 8 clearly shows this adsorbed and absorbed chlorine is not participating in phosgene production. These differences between the two activated carbons are thought to be real and distinct. They are not attributed to changes in the reactor formats as discussed in Section 3.2, which can affect absolute values but not systematic trends.

Equation (2) expresses the equilibrium condition as described by Equation (1) in terms of forward and backward rate coefficients (k_f and k_b).

$$K_2 = \frac{k_f}{k_b} \tag{2}$$

It appears that whereas k_b describes a pathway that is active for Donau Supersorbon K40 beyond the point of total chlorine consumption and over the temperature range 393–423 K, it is not observable for Norit RX3 Extra over the higher temperature range of 473–504 K. This scenario indicates the dynamics of the chlorine interchange reaction (Equation 1) on the two materials to be different, which is attributed to differences in the active site distributions of the two catalysts. Indeed, Figure 8 shows Norit RX3 Extra to be a more direct substrate for analysis, as once Cl_2 is completely consumed, $COCl_2$ formation plateaus.

The modest differences in performance that were noted between the two materials requires the reaction scheme, developed exclusively using Donau Supersorbon K40 (Scheme 1), to be amended to better represent the phosgene synthesis performance of both Donau Supersorbon K40 and Norit RX3 Extra. Scheme 2 presents the newly modified series of elementary reactions thought to be contributing to phosgene synthesis over activated carbons.

The format of the revised reaction model (Scheme 2) is now considered. Firstly, the diffusion of chlorine on the activated carbon surface is now designated as k_3, which is split into k_{3a} and k_{3b} that denote the movement of chlorine from the nonreactive to the reactive site and the reverse process respectively. Over the temperature range 393–423 K, k_{3a} is active for Donau Supersorbon K40 but a distinct role for the $Cl''_{(ad)} \rightarrow Cl'_{(ad)}$ conversion is not observable for Norit RX3 Extra, which includes the range 473–504 K for which Figure 8 shows significant chlorine retention.

Furthermore, the adsorption of chlorine to the activated carbon surface is now split into k_1 and k_2. The correction is necessary because the original scheme indicated chlorine to adsorb sequentially into the reactive site and then to the nonreactive

site, which may well not be the case. Finally, k_4 has been added to represent the desorption of phosgene from the catalyst into the gas phase. In summary, it is proposed that Scheme 2 provides a framework that can reasonably explain the performance of both Donau Supersorbon K40 and Norit RX3 Extra during reagent turnover to selectively produce the valuable phosgene product. This is a progressive step concerning developing a mechanistic understanding of phosgene synthesis catalysis over activated carbons. Studies to further interrogate the generic nature of Scheme 2 constitute work in progress.

4. Conclusions

Norit RX3 Extra has been selected as a different activated carbon for examination of a previously proposed reaction scheme for phosgene synthesis catalysis that was developed by using Donau Supersorbon K40 as a substrate. The following conclusions can be drawn:

- Physical characterization of the commercial grade Norit RX3 Extra had established that the sample investigated is within specification of previously published reports of this widely used material and, therefore, subsequent results on phosgene synthesis catalysis over this material should be reproducible by other researchers.
- The reaction profile for the co-feeding of carbon monoxide and chlorine over the catalyst at 323 K (Figure 3) showed the steady-state production of phosgene to be rapidly achieved (~0.33 mmol/min/g(cat)), with phosgene as the only product and no catalyst deactivation was evident.
- The mass balance plots for reaction at 323 K show a closed carbon mass (Figure 4), but the chlorine mass balance plot (Figure 5) revealed a small and continuous retention of chlorine, which was corroborated by postreaction SEM/EDX analysis. Under comparable conditions, the extent of chlorine retention was less than that reported for Donau Supersorbon K40.
- Temperature-programmed reaction over the range 333–504 K had returned a relatively simple reaction profile with the concomitant consumption of reagents and exclusive formation of product (Figure 8). Under comparable conditions, complete chlorine consumption was observed at 473 K, rather than the 393 K reported for Donau Supersorbon K40.
- The carbon mass balance plot (Figure 9) for the temperature programmed measurements have indicated a closed carbon mass balance for $T \leq 457$ K, but for $T \geq 473$ K a small carbon imbalance resulted. In contrast, the chlorine mass balance data (Figure 10) showed increasing chlorine retention as a function of increasing temperature from 333 K onward, with the deficit at 504 K representing a 11.3% of the catalyst mass normalized chlorine flow rate (A0). No catalyst deactivation was observed over the temperature and time range studied.
- In contrast to previously reported outcomes for Donau Supersorbon K40, the phosgene formation rate plateaued at temperatures corresponding to complete chlorine conversion (Figure 8). This outcome was interpreted as indicating that, under the stated conditions, Norit RX3 Extra was provided no transfer from inactive retained chlorine atoms (Cl(ad)″) to active adsorbed chlorine atoms (Cl(ad)′), Equation (1).
- A modified reaction scheme is proposed to account for phosgene synthesis from the reaction of carbon monoxide and chlorine over Donau Supersorbon K40 and Norit RX3 Extra (Scheme 2).

Supporting Information

Physical characterization of Norit RX3 extra: Figure S1, Thermogravimetric and derivative gravimetric analysis; Figure S2, Energy dispersive x-ray spectrum of the as-received Norit RX3 extra; Figure S3, X-Ray photoelectron spectra; Figure S4, Nitrogen adsorption isotherm; Figure S5: Raman spectrum; Figure S6, Powder x-ray diffractogram; Figure S7, Energy dispersive x-ray spectrum of postreaction sample.

Author Contributions

R. Hughes: Methodology, validation, formal analysis, investigation, resources, data curation, writing—original draft, writing—review and editing, Visualization; **P.R. Davies**: validation, formal analysis, writing—review and editing; **C. Brennan**: Validation, formal analysis, **D. Lennon**: Conceptualization, methodology, resources, writing—review and editing, supervision, project administration, funding acquisition.

Acknowledgments

We gratefully acknowledge the EPSRC for the provision of a Ph.D. studentship (RH, EP/R513222/1 and EP/T517896/1). Mr. Andy Monaghan (TGA/DTG, Raman, UoG), Mr. Jim Gallagher (SEM/EDX, UoG), Dr. Chris Kelly (BET, UoG), Mr. Christos Ballas (BET, UoG), Dr. Claire Wilson (XRD, UoG), Mr. Raman Dosanjh (XRD, UoG), and Dr. Shaoliang Guan (XPS, HarwellXPS, operated by Cardiff University and UCL under contract number PR16195) thanked the provision of technical assistance connected the catalyst characterization measurements. The referees of this article are also thanked for their contributions to the final manuscript.

Conflict of Interests

The authors declare no conflict of interest.

Data Availability Statement

The data that support the findings of this study, including spectroscopic datasets, are available at the University of Glasgow Library [DOI: https://doi.org/10.5525/gla.researchdata.1846].

Keywords: Activated carbon · Mass balance · Microreactor · Phosgene synthesis catalysis

[1] C. J. Mitchell, W. van der Borden, K. van der Velde, M. Smit, R. Scheringa, K. Ahrika, D. H. Jones, *Catal. Sci. Technol.* **2012**, *2*, 2109.
[2] T. A. Ryan, C. Ryan, E. A. Seddon, K. R. Seddon, *Phosgene and Related Carbonyl Halides*, Elseiver, Amsterdam, **1996**.
[3] L. Cotarca, H. Ekert, *Phosgenations–A Handbook*, Wiley VCH, Weinheim **2006**.
[4] L. Cotarca, C. Lange, K. Meurer, J. Pauluhn, in *Ullmann's Encyclopedia of Industrial Chemistry*, Wiley-VCH Verlag GmbH & Co. KGaA, Weinheim, Germany **2019**, pp. 1–30.
[5] P. Voßnacker, A. Wüst, T. Keilhack, C. Müller, S. Steinhauer, H. Beckers, S. Yogendra, Y. Schiesser, R. Weber, M. Reimann, R. Müller, M. Kaupp, S. Riedel, *Sci. Adv.* **2021**, *7*, https://doi/org/10.1126/sciadv.abj5186.
[6] S.-H. Pyo, P. Persson, M. A. Mollaahmad, K. Sörensen, S. Lundmark, R. Hatti-Kaul, *Pure Appl. Chem.* **2011**, *84*, 637–661.
[7] R. Hughes, G. E. Rossi, D. Lennon, *React. Chem. Eng.* **2023**, *8*, 3150–3161.
[8] J. Pauluhn, *Toxicology* **2021**, *450*, 152682.
[9] E. Fuente, J. A. Menéndez, M. A. Díez, D. Suárez, M. A. Montes-Morán, *J. Phys. Chem. B* **2003**, *107*, 6350–6359.
[10] A. M. McCullagh, E. K. Gibson, S. F. Parker, K. Refson, D. Lennon, *Phys. Chem. Chem. Phys.* **2023**, *25*, 25993–26005.
[11] A. M. McCullagh, A. L. Davidson, C. E. Ballas, C. How, D. A. MacLaren, C. Boulho, C. Brennan, D. Lennon, *Catal. Today* **2024**, *442*, 114933.
[12] C. Potter, S. Baron, *Chem. Eng. Prog.* **1951**, *47*, 473–479.
[13] S. Baron, The Kinetics of the Catalytic Formation of Phosgene, Doctor of Philosophy, Columbia University **1950**.
[14] Z. CSŰRÖS, R. Soos, I. Petneházy, G. T. Szabó, *Period. Polytech. Chem. Eng.* **1970**, *14*, 3–11.
[15] E. N. Shapatina, V. L. Kuchaev, B. E. Pen'kovol, M. I. Temkin, *Kinetika I Kataliz* **1974**, *17*, 644–652.
[16] E. N. Shapatina, V. L. Kuchaev, M. I. Temkin, *Kinetika I Kataliz* **1977**, *18*, 968–972.
[17] E. N. Shapatina, V. L. Kuchaev, M. I. Temkin, *Kinetika I Kataliz* **1979**, *20*, 1183–1187.
[18] W. V. Cicha, L. E. Manzer, *WO1998000364A1* **1998**.
[19] K. Urakawa, K. S. Ashida, *JPH0629129B2* **1988**.
[20] W. V. Cicha, L. E. Manzer, *US 6,054,612* **2000**.
[21] R. P. Obrecht, *US 4,231,959* **1980**.
[22] H. Sauer, H. P. Porkert, D. Liebsch, *US 4, 764, 308* **1988**.
[23] N. Kunisi, N. Murai, H. Kusama, *EP 0 796 819 B1* **1997**.
[24] L. Abrams, W. V. Cicha, L. E. Manzer, S. Subramoney, **2000**, pp. 455–460.
[25] S. K. Ajmera, M. W. Losey, K. F. Jensen, M. A. Schmidt, *AIChE J.* **2001**, *47*, 1639–1647.
[26] N. K. Gupta, A. Pashigreva, E. A. Pidko, E. J. M. Hensen, L. Mleczko, S. Roggan, E. E. Ember, J. A. Lercher, *Angew. Chem., Int. Ed.* **2016**, *55*, 1728–1732.
[27] G. Centi, K. Barbera, S. Perathoner, N. K. Gupta, E. E. Ember, J. A. Lercher, *ChemCatChem* **2015**, *7*, 3036–3046.
[28] N. K. Gupta, B. Peng, G. L. Haller, E. E. Ember, J. A. Lercher, *ACS Catal.* **2016**, *6*, 5843–5855.
[29] A. Bähr, G.-H. Moon, J. Diedenhoven, J. Kiecherer, E. Barth, H. Tüysüz, *Chem. Ing. Tech.* **2018**, *90*, 1513–1519.
[30] A. Bähr, J. Diedenhoven, H. Tüysüz, *Chem. Ing. Tech.* **2020**, *92*, 1508–1513.
[31] G. E. Rossi, J. M. Winfield, N. Meyer, D. H. Jones, R. H. Carr, D. Lennon, *Ind. Eng. Chem. Res.* **2021**, *60*, 3363–3373.
[32] G. E. Rossi, J. M. Winfield, C. J. Mitchell, W. van der Borden, K. van der Velde, R. H. Carr, D. Lennon, *Appl. Catal. A Gen.* **2020**, *594*, 117467.
[33] G. E. Rossi, J. M. Winfield, C. J. Mitchell, N. Meyer, D. H. Jones, R. H. Carr, D. Lennon, *Appl. Catal. A Gen.* **2020**, *602*, 117688.
[34] G. E. Rossi, J. M. Winfield, N. Meyer, D. H. Jones, R. H. Carr, D. Lennon, *Appl. Catal. A Gen.* **2021**, *609*, 117900.
[35] N. Fairley, V. Fernandez, M. Richard-Plouet, C. Guillot-Deudon, J. Walton, E. Smith, D. Flahaut, M. Greiner, M. Biesinger, S. Tougaard, D. Morgan, J. Baltrusaitis, *Appl. Surf. Sci. Adv.* **2021**, *5*, 100112.
[36] M. Bodenstein, *Chem. Rev.* **1930**, *7*, 225–229.
[37] K.-D. Henning, H. von Kienle, in *Ullmann's Encyclopedia of Industrial Chemistry*, Wiley-VCH Verlag GmbH & Co. KGaA, Weinheim, Germany **2010**.
[38] F. Duarte, F. J. Maldonado-Hódar, L. M. Madeira, *Appl. Catal. B* **2013**, *129*, 264–272.
[39] M. Cordoba, C. Miranda, C. Lederhos, F. Coloma-Pascual, A. Ardila, G. Fuentes, Y. Pouilloux, A. Ramírez, *Catalysts* **2017**, *7*, 384.
[40] M. S. Shafeeyan, W. M. A. W. Daud, A. Houshmand, A. Shamiri, *J. Anal. Appl. Pyrolysis* **2010**, *89*, 143–151.
[41] J. González, M.del C. Ruiz, A. Bohé, D. Pasquevich, *Carbon N Y* **1999**, *37*, 1979–1988.
[42] C. R. Hall, R. J. Holmes, *Carbon N Y* **1992**, *30*, 173–176.
[43] Y. Leng, in *Materials Characterization: Introduction to Microscopic and Spectroscopic Methods, 2nd ed.*, Wiley KGaA, Weinheim, Germany **2013**, pp. 191–219.
[44] J. L. Figueiredo, M. F. R. Pereira, M. M. A. Freitas, J. J. M. Órfão, *Carbon N Y* **1999**, *37*, 1379–1389.
[45] A. Malaika, P. Rechnia, B. Krzyżyńska, A. Tolińska, A. Kawałko, M. Kozłowski, *Appl. Catal. A Gen.* **2013**, *452*, 39–47.
[46] H. Tobias, A. Soffer, *Carbon N Y* **1985**, *23*, 281–289.
[47] J. Hollas, in *Modern Spectroscopy 4th ed.*, Wiley, West Sussex, England **2004**, pp. 289–335.
[48] A. M. Puziy, O. I. Poddubnaya, R. P. Socha, J. Gurgul, M. Wisniewski, *Carbon N Y* **2008**, *46*, 2113–2123.
[49] S. Biniak, G. Szymański, J. Siedlewski, A. Świątkowski, *Carbon N Y* **1997**, *35*, 1799–1810.
[50] M. Weller, T. Overton, J. Rourke, F. Armstrong, in *Inorg Chem*, Oxford University Press, Oxford **2014**, pp. 381–407.
[51] K. Sing, *Colloids Surf., A* **2001**, *187*, 3–9.
[52] P. Schneider, *Appl. Catal. A Gen.* **1995**, *129*, 157–165.
[53] I. Mesquita, L. C. Matos, F. Duarte, F. J. Maldonado-Hódar, A. Mendes, L. M. Madeira, *J. Hazard. Mater.* **2012**, *237*, 30–37.
[54] S. K. Henninger, M. Schicktanz, P. P. C. Hügenell, H. Sievers, H.-M. Henning, *Int. J. Refrig.* **2012**, *35*, 543–553.
[55] A. Malaika, M. Kozłowski, *Int. J. Hydrogen Energy* **2010**, *35*, 10302–10310.
[56] F. Duarte, F. J. Maldonado-Hódar, L. M. Madeira, *Appl. Catal. B* **2011**, *103*, 109–115.
[57] J. P. S. Sousa, M. F. R. Pereira, J. L. Figueiredo, *Fuel Process. Technol.* **2013**, *106*, 727–733.
[58] Q. Chang, W. Lin, W. Ying, *J. Hazard. Mater.* **2010**, *184*, 515–522.
[59] J. P. S. Sousa, M. F. R. Pereira, J. L. Figueiredo, *Catal. Today* **2011**, *176*, 383–387.
[60] M. Godino-Ojer, L. Milla-Diez, I. Matos, C. J. Durán-Valle, M. Bernardo, I. M. Fonseca, E. Pérez Mayoral, *ChemCatChem* **2018**, *10*, 5215–5223.
[61] M. Quiroga, D. Liprandi, P. L'Argentière, E. Cagnola, *J. Chem. Technol. Biotechnol.* **2005**, *80*, 158–163.
[62] C. Xu, A. S. Teja, *Appl Catal A Gen* **2008**, *348*, 251–256.
[63] A. C. Ferrari, *Solid State Commun.* **2007**, *143*, 47–57.
[64] A. C. Ferrari, J. Robertson, *Phys. Rev. B* **2000**, *61*, 14095–14107.
[65] A. C. Ferrari, J. C. Meyer, V. Scardaci, C. Casiraghi, M. Lazzeri, F. Mauri, S. Piscanec, D. Jiang, K. S. Novoselov, S. Roth, A. K. Geim, *Phys. Rev. Lett.* **2006**, *97*, 187401.
[66] R. Sharabi, Y. H. Wijsboom, N. Borchtchoukova, G. Finkelshtain, L. Elbaz, *J. Power Sources* **2016**, *335*, 56–64.
[67] E. Kordouli, C.h. Kordulis, A. Lycourghiotis, R. Cole, P. T. Vasudevan, B. Pawelec, J. L. G. Fierro, *Mol. Catal.* **2017**, *441*, 209–220.
[68] F. Tuinstra, J. L. Koenig, *J. Chem. Phys.* **1970**, *53*, 1126–1130.
[69] Y. Leng, in *Materials Characterization: Introduction to Microscopic and Spectroscopic Methods 2nd ed.*, Wiley, Weinheim, Germany **2013**, pp. 47–82.
[70] F. Duarte, V. Morais, F. J. Maldonado-Hódar, L. M. Madeira, *Chem. Eng. J.* **2013**, *232*, 34–41.
[71] A. M. Ricks, A. D. Brathwaite, M. A. Duncan, *J. Phys. Chem. A* **2013**, *117*, 11490–11498.
[72] D. Chao, Z. Dongke, Z. Yujie, L.i Chaoqun, W. Wenbo, Z. Hongke, X.u Dan, L.i Chong, S. Jie, *WO2021035769A1* **2021**.
[73] H. Takahashi, F. Onuma, Y. Sasaki, *JP5667253B2* **2013**.
[74] F. A. Via, G. L. Soloveichik, P. G. Kosky, W. V. Cicha, *US 6, 399, 823 B1* **2002**.
[75] I. Grinvald, I. Kalagaev, A. Petukhov, A. Vorotyntsev, R. Kapustin, *Struct. Chem.* **2019**, *30*, 1659–1664.
[76] C. Perego, S. Peratello, *Catal. Today* **1999**, *52*, 133–145.

Manuscript received: June 28, 2024
Revised manuscript received: October 22, 2024
Accepted manuscript online: December 02, 2024
Version of record online: December 20, 2024